From QCD Instantons at HERA to Electroweak $B + L$ Violation at VLHC

Andreas Ringwald[*]

Deutsches Elektronen-Synchrotron DESY, Notkestraße 85, D–22607 Hamburg, Germany
E-mail: `andreas.ringwald@desy.de`

ABSTRACT: This review emphasizes the close analogy between hard QCD instanton-induced chirality violating processes in deep-inelastic scattering and electroweak instanton-induced baryon plus lepton number $(B + L)$ violating processes in Quantum Flavor Dynamics (QFD). Recent information about QCD instantons, both from lattice simulations and from the H1 experiment at HERA, can be used to learn about the fate of electroweak $B+L$ violation at future high energy colliders in the hundreds of TeV regime, such as the projected Very Large Hadron Collider (VLHC). The cross-sections turn out to be unobservably small in a conservative fiducial kinematical region inferred from the above mentioned QCD–QFD analogy. An extrapolation – still compatible with lattice results and HERA – beyond this conservative limit indicates possible observability at VLHC.

1. Introduction

Over the last decades we have witnessed the remarkable success of the Standard Model of electroweak (Quantum Flavor Dynamics (QFD)) and strong (QCD) interactions. This success is largely based on the possibility to apply ordinary perturbation theory to the calculation of hard, short-distance dominated scattering processes, since the relevant gauge couplings are small.

There are certain processes, however, which fundamentally can not be described by ordinary perturbation theory, no matter how small the gauge coupling is. These processes are associated with axial anomalies [1] and manifest themselves as anomalous violation of baryon plus lepton number $(B+L)$ in QFD and chirality (Q_5) in QCD [2]. They are induced by topological fluctuations of the non-Abelian gauge fields, notably by instantons [3].

A number of non-perturbative issues in the Standard Model can be understood in terms of such topological fluctuations and the associated anomalous processes. On the

---

[*]Speaker.

one hand, QCD instantons seem to play an important role in various long-distance aspects of QCD, such as providing a possible solution to the axial $U(1)$ problem [2] or being at work in $SU(n_f)$ chiral symmetry breaking [4, 5]. In QFD, on the other hand, similar topological fluctuations of the gauge fields and the associated $B + L$ violating processes are very important at high temperatures [6] and have therefore a crucial impact on the evolution of the baryon and lepton asymmetries of the universe [7].

A related question is whether manifestations of such topological fluctuations may be directly observed in high-energy scattering processes. It has been raised originally in the late eighties in the context of QFD [8, 9]. But, despite considerable theoretical [10, 11, 12, 13] and phenomenological [14, 15, 16] efforts, the actual size of the cross-sections in the relevant, tens of TeV energy regime was never established (for reviews, see Refs. [7, 17]). Meanwhile, the focus switched to quite analogous QCD instanton-induced hard scattering processes in deep-inelastic scattering [18, 19], which are calculable from first principles within instanton-perturbation theory [20], yield sizeable rates for observable final state signatures in the fiducial regime of the latter [21, 22, 23, 24, 25], and are actively searched for at HERA [26]. Moreover, it has been recognized recently that larger-size QCD instantons, beyond the semi-classical, instanton-perturbative regime, may well be responsible for the bulk of inelastic hadronic processes and build up soft diffractive scattering [27].

In this review, we emphasize the close analogy of QFD and hard QCD instanton-induced processes in deep-inelastic scattering [19] (Sect. 2) and recall the recent information about the latter both from lattice simulations [22, 25, 28] and from the H1 experiment at HERA [26] (Sect. 3). We summarize a recent state of the art evaluation of QFD instanton-induced parton-parton cross-sections [29] (Sect. 4), as relevant at future high energy colliders in the hundreds of TeV regime, such as the projected Eurasian Long Intersecting Storage Ring (ELOISATRON) [30] or the Very Large Hadron Collider (VLHC) [31]. The implications of the lattice and HERA results – via the above mentioned QFD–QCD analogy – for the fate of electroweak $B + L$ violation in high energy collisions are discussed.

2. Instanton-induced hard scattering processes

2.1 Generalities

Instantons [2, 3, 32] are minima of the classical Euclidean Yang-Mills action, localized in space and Euclidean time, with unit topological charge (Pontryagin index) $Q = 1$. In Minkowski space-time, instantons describe tunneling transitions between classically degenerate, topologically inequivalent vacua, differing in their winding number (Chern-Simons number) by one unit, $\triangle N_{\rm CS} = Q = 1$ [33]. The corresponding energy barrier ("sphaleron energy" [34]), under which the instantons tunnel, is inversely proportional to $\alpha_g \equiv g^2/(4\pi)$, the fine-structure constant of the relevant gauge theory, and the effective instanton-size $\rho_{\rm eff}$,

$$M_{\rm sp} \sim \frac{\pi}{\alpha_g \, \rho_{\rm eff}} \sim \begin{cases} \pi \frac{M_W}{\alpha_W} \sim 10 \text{ TeV} & \text{in QFD [34]}, \\ \mathcal{Q} & \text{in QCD [19, 20, 21]}, \end{cases} \qquad (2.1)$$

where $\mathcal{Q}$ is a large momentum transfer e.g. in deep-inelastic scattering (DIS), which should be taken $\gtrsim 10$ GeV in order to be in the semi-classical, instanton-perturbative

regime [20, 21, 22, 25]. Axial anomalies [1] force instanton-induced hard scattering processes to be always associated with anomalous fermion-number violation [2], in particular $B + L$ violation,

$$\triangle B = \triangle L = -n_{\text{gen}} Q, \tag{2.2}$$

in the case of QFD with $n_{\text{gen}} = 3$ fermion generations, and chirality violation,

$$\triangle Q_5 = 2 n_f Q, \tag{2.3}$$

in the case of QCD with typically $n_f = 3$ light quark flavors.
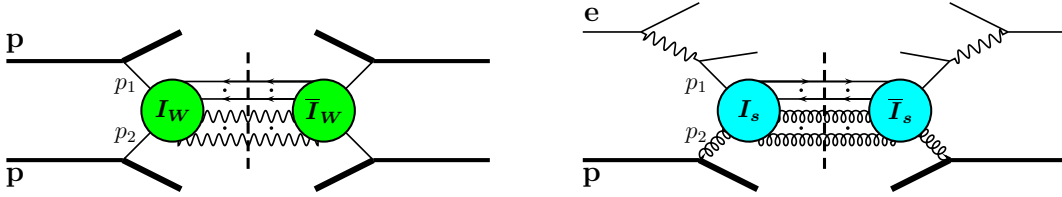
Figure 1: Illustration of a QFD instanton-induced process in proton-proton scattering (*left*) and of a QCD instanton-induced process in deep-inelastic electron-proton scattering (*right*) (from [29]).

In instanton-perturbation theory – the semi-classical expansion of the corresponding path integral expressions about the instanton solution – instanton-induced total cross-sections for hard parton-parton (p_1-p_2) scattering processes (cf. Fig. 1) are given in terms of an integral over the instanton-anti-instanton[1] ($I\bar{I}$) collective coordinates (sizes $\rho, \bar{\rho}$, $I\bar{I}$ distance R, relative color orientation U) [21] (see also [11, 12, 13, 29, 35, 36])

$$\hat{\sigma}^{(I)}_{\text{p}_1\text{p}_2} = \frac{1}{2 p_1 \cdot p_2} \, \text{Im} \int \mathrm{d}^4 R \, \mathrm{e}^{\mathrm{i}\, (p_1 + p_2) \cdot R} \tag{2.4}$$

$$\times \int_0^\infty \mathrm{d}\rho \int_0^\infty \mathrm{d}\overline{\rho} \, D(\rho) \, D(\overline{\rho}) \int \mathrm{d}U \, \mathrm{e}^{-\frac{4\pi}{\alpha_g}\Omega\left(U, \frac{R^2}{\rho\bar{\rho}}, \frac{\bar{\rho}}{\rho}, \dots\right)} \left[\omega\left(U, \frac{R^2}{\rho\bar{\rho}}, \frac{\bar{\rho}}{\rho}, \dots\right)\right]^{n_{\text{fin}}}$$

$$\times F\left(\sqrt{-p_1^2}\, \rho\right) F\left(\sqrt{-p_1^2}\, \overline{\rho}\right) F\left(\sqrt{-p_2^2}\, \rho\right) F\left(\sqrt{-p_2^2}\, \overline{\rho}\right) \dots .$$

Here, the main building blocks are *i)* the instanton-size distribution $D(\rho)$, *ii)* the function Ω, which takes into account the exponentiation of the production of $\mathcal{O}(1/\alpha_g)$ (gauge) bosons [9, 11] and can be identified with the $I\bar{I}$-interaction defined via the valley method [12, 37, 38, 39], and *iii)* the function ω, whose explicit form can be found in Refs. [13, 21] and which summarizes the effects of final-state fermions. Their number n_{fin} is related to the number n_{in} of initial-state fermions via the anomaly,

$$n_{\text{fin}} + n_{\text{in}} \equiv n_{\text{tot}} \equiv \begin{cases} 4\, n_{\text{gen}} \; = 12 & \text{in QFD}, \\ 2\, n_f & \text{in QCD}. \end{cases} \tag{2.5}$$

---

[1]Both an instanton and an anti-instanton enter here, since the cross-section (2.4) has been written as a discontinuity of the $p_1 p_2$ forward elastic scattering amplitude in the $I\bar{I}$-background (cf. Fig. 1). Alternatively, one may calculate the cross-section by taking the modulus squared of amplitudes in the single instanton-background.

With each initial-state parton p, there is an associated "form factor" [20, 21],

$$F(x) = x\,K_1(x) \begin{cases} \simeq \sqrt{\pi/(2\,x)}\,\exp(-x) & \text{for } x \gg 1, \\ = 1 & \text{for } x = 0. \end{cases} \tag{2.6}$$

The dots in Eq. (2.4) stand for further known smooth factors [21].

Let us elaborate further on the quantities mentioned under *i)* and *ii)*.

Ad i) The instanton-size distribution $D(\rho)$ is known in instanton-perturbation theory, $\alpha_g(\rho^{-1}) \ll 1$, up to two-loop renormalization group invariance [2, 40, 41]. In QCD, the loop corrections are sizeable in the phenomenologically interesting range [21, 22]. For a qualitative discussion, however, the one-loop expression for the size distribution,

$$D(\rho) = \frac{d}{\rho^5}\left(\frac{2\pi}{\alpha_g(\mu)}\right)^{2\,N_c} (\mu\,\rho)^{\beta_0}\, \mathrm{e}^{-\frac{2\pi}{\alpha_g(\mu)}\,S^{(I)}}, \tag{2.7}$$

suffices, which, moreover, is numerically adequate for the case of QFD because of its weak coupling, $\alpha_W(M_W) \equiv \alpha(M_W)/\sin^2\hat{\theta}(M_W) = 0.033819(23)$ [42]. In Eq. (2.7),

$$\beta_0 = \frac{11}{3}\,N_c - \frac{1}{6}\,n_s - \frac{1}{3}\,n_{\text{tot}} = \begin{cases} 19/6 & \text{in QFD } (N_c = 2, n_s = 1, n_{\text{tot}} = 12), \\ 11 - 2\,n_f/3 & \text{in QCD } (N_c = 3, n_s = 0, n_{\text{tot}} = 2\,n_f), \end{cases} \tag{2.8}$$

denotes the first coefficient in the β function,

$$S^{(I)} = \begin{cases} 1 + \frac{1}{2}\,M_W^2\,\rho^2 + \mathcal{O}\left(M_W^4\,\rho^4\ln(M_W\,\rho)\right) & \text{in QFD [2, 32]}, \\ 1 & \text{in QCD [3]}, \end{cases} \tag{2.9}$$

the instanton action, μ the renormalization scale, and d a scheme-dependent constant, which reads in the $\overline{\text{MS}}$ scheme [43],

$$d_{\overline{\text{MS}}} = \frac{2\,\mathrm{e}^{5/6}}{\pi^2\,(N_c-1)!(N_c-2)!}\,\mathrm{e}^{-1.511374\,N_c + 0.291746\,(n_{\text{tot}}+n_s)/2}. \tag{2.10}$$

The quite different ρ dependence of the size distribution (2.7) for QFD and QCD has important consequences for the predictivity of instanton-induced subprocess cross-sections (2.4). The validity of instanton-perturbation theory requires instantons of small enough size, such that $\alpha_g(\rho^{-1}) \ll 1$. In QFD, this is guaranteed by the exponential decrease $\propto \exp(-\pi\,M_W^2\,\rho^2/\alpha_W)$ (cf. (2.9)) of the size distribution (2.7) for $\rho > \rho_{\max} = 0.13/M_W$ (cf. Fig. 2 (left)). Therefore, the relevant contributions to the size integrals in (2.4) arise consistently from the perturbative region ($\alpha_W(\rho^{-1}) \ll 1$) even if both initial partons are on-shell, $p_1^2 \approx p_2^2 \approx 0$, as relevant for electroweak instanton-induced processes, e.g. in proton-proton scattering (cf. Fig. 1 (left)).

In QCD, on the other hand, the perturbative expression (2.7) for the size distribution behaves power-like, $\propto \rho^{\beta_0 - 5}$ (cf. Fig. 2 (right)). This behavior generically causes the dominant contributions to observables like the cross-section (2.4) to originate from large $\rho \sim \Lambda^{-1} \Rightarrow \alpha_s(\rho^{-1}) \sim 1$ and thus tends to spoil the applicability of instanton-perturbation theory. Deep-inelastic scattering, however, offers a unique opportunity to test the predictions of instanton-perturbation theory from first principles [20, 21, 22, 23, 24, 25]. This
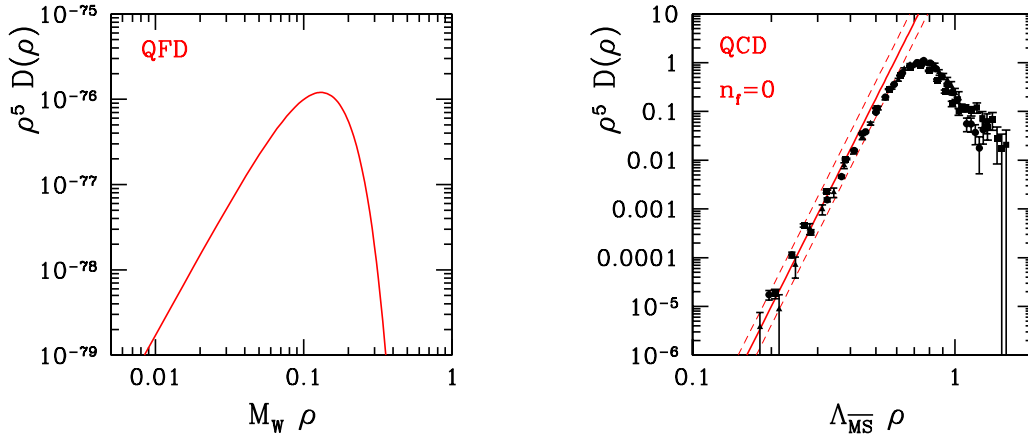
Figure 2: Instanton-size distributions as predicted in instanton-perturbation theory (solid lines) in QFD (left) and quenched ($n_f = 0$) QCD (right). For QCD (right), the two-loop renormalization group invariant prediction for the size distribution from Ref. [41] together with the 3-loop form of $\alpha_{\overline{\mathrm{MS}}}$, with $\Lambda_{\overline{\mathrm{MS}}}^{(0)} = 238 \pm 19$ MeV from the ALPHA collaboration [44], was used. The error band (dashed lines) results from the errors in $\Lambda_{\overline{\mathrm{MS}}}$ and a variation of $\mu = 1 \div 10$ GeV. *Left:* Towards large sizes, the QFD instanton size distribution decreases exponentially due to the Higgs mechanism. *Right:* For large sizes, the QCD instanton size distribution, as determined from recent high-quality lattice data from UKQCD [28][2], appears to decrease exponentially, $\propto \exp(-c\rho^2)$ [22, 49], similar to the QFD size distribution (left), but unlike the instanton-perturbative prediction (solid). For small sizes, on the other hand, one observes a remarkable agreement with the predictions from instanton-perturbation theory (solid) [22, 25].

can be understood as follows. In deep-inelastic electron-proton scattering, the virtual photon splits into a quark and an antiquark, one of which, p_1 say, enters the instanton subprocess (cf. Fig. 1 (right)). This parton carries a space-like virtuality $Q'^2 \equiv -p_1^2 \geq 0$, which can be made sufficiently large by kinematical cuts on the final state. In this hard-scattering regime the contribution of large instantons to the integrals is suppressed by the exponential form factors (2.6) in (2.4), $\propto e^{-Q'(\rho + \bar{\rho})}$, and instanton-perturbation theory is reliable [20, 21]. In this connection it is quite welcome that lattice data on the instanton content of the quenched ($n_f = 0$) QCD vacuum [28][2] can be used to infer the region of validity of instanton-perturbation theory for $D(\rho)$ [22, 25]: As illustrated in Fig. 2 (right), there is very good agreement for $\Lambda_{\overline{\mathrm{MS}}}\, \rho \lesssim 0.42$.

    Ad ii) A further basic building block of instanton-induced cross-sections (2.4) is the function $\Omega(U, R^2/(\rho\bar{\rho}), \bar{\rho}/\rho)$, appearing in the exponent with a large numerical coefficient $4\pi/\alpha_g$. It summarizes the effects of the $\mathcal{O}(1/\alpha_g)$ final-state (gauge) bosons, mainly W's and Z's in the case of QFD and gluons in the case of QCD. Within strict instanton-perturbation theory, it is given in form of a perturbative expansion [11, 21, 39] for large $I\bar{I}$-distance squared R^2. Beyond this expansion, one may identify Ω with the interaction

---

[2]For further, qualitative similar lattice data, see Refs. [45, 46] and the reviews [47, 48].

between an instanton and an anti-instanton, which may be systematically evaluated by means of the so-called $I\bar{I}$-valley method [37]. The corresponding interaction has been found analytically for the case of pure $SU(2)$ gauge theory[3] [12, 38],

$$\Omega_g = \Omega_0 + \Omega_1 \, u_0^2 + \Omega_2 \, u_0^4 \,, \tag{2.11}$$

with

$$\Omega_0 = 2 \, \frac{z^4 - 2z^2 + 1 + 2\,(1 - z^2)\ln z}{(z^2 - 1)^3} \,,$$

$$\Omega_1 = -8 \, \frac{z^4 - z^2 + (1 - 3\,z^2)\ln z}{(z^2 - 1)^3} \,, \tag{2.12}$$

$$\Omega_2 = -16 \, \frac{z^2 - 1 - (1 + z^2)\ln z}{(z^2 - 1)^3} \,.$$

Due to conformal invariance of classical pure Yang-Mills theory, it depends on the sizes ρ, $\bar{\rho}$, and the $I\bar{I}$-distance R only through the "conformal separation",

$$z = \frac{1}{2} \left(\xi + \sqrt{\xi^2 - 4} \right) \,, \qquad \xi = \frac{R^2}{\rho\bar{\rho}} + \frac{\bar{\rho}}{\rho} + \frac{\rho}{\bar{\rho}} \geq 2 \,, \tag{2.13}$$

and on the relative color orientation[3] $U = u_0 + i\,\sigma^k u_k$, with $u_0^2 + u^k u_k = 1$, only through u_0.

In the weak coupling regime, $\alpha_g \ll 1$, $I\bar{I}$-pairs with the most attractive relative orientation, $U = 1$, give the dominant contribution to the cross-section (2.4). For this relative orientation, the $I\bar{I}$-valley represents a gauge field configuration of steepest descent interpolating between an infinitely separated $I\bar{I}$-pair, corresponding to twice the instanton action, $S^{(I\bar{I})} = 2\,[1 + \Omega_g(U = 1, \xi = \infty)] = 2$, and a strongly overlapping one, annihilating to the perturbative vacuum at $\xi = 2$ ($R = 0, \rho = \bar{\rho}$), corresponding to vanishing action $S^{(I\bar{I})} = 2\,[1 + \Omega_g(U = 1, \xi = 2)] = 0$ (cf. Fig. 3 (left)). Thus, near $\xi \approx 2$, the semi-classical approximation based on the $I\bar{I}$-valley breaks down and no reliable non-perturbative information can be extracted from it.

In this connection one may exploit again high-quality lattice data [28] on the $I\bar{I}$-distance distribution in quenched QCD to estimate the fiducial region in ξ or more specifically in $R/\langle\rho\rangle$, where $\langle\rho\rangle \approx 0.5$ fm is the average instanton/anti-instanton size measured on the lattice (cf. Fig. 2 (right)). Good agreement with the predictions from instanton-perturbation theory is found for $R/\langle\rho\rangle \gtrsim 1.0 \div 1.05$ [22, 25] (cf. Fig. 3 (right)). There are, however, remaining ambiguities in this case. *a)* The integrations over ρ, $\bar{\rho}$ in the $I\bar{I}$-distance distribution $\mathrm{d}n_{I\bar{I}}/(\mathrm{d}^4x\,\mathrm{d}^4R)$ imply significant contributions also from larger instantons with $0.42 \lesssim \Lambda_{\overline{\mathrm{MS}}}\,\rho, \Lambda_{\overline{\mathrm{MS}}}\,\bar{\rho} \lesssim 1$, outside the region of instanton-perturbation theory. A more differential lattice measurement of the distance distribution, $\mathrm{d}n_{I\bar{I}}/(\mathrm{d}^4x\,\mathrm{d}^4R\,\mathrm{d}\rho\,\mathrm{d}\bar{\rho})$, which includes also differentials with respect to the sizes ρ and $\bar{\rho}$, and eventually a test of its conformal properties would resolve these theoretical ambiguities. *b)* At small $I\bar{I}$-separation

---

[3]For the embedding of the $SU(2)$ $I\bar{I}$-valley into $SU(3)$, see e.g. Ref. [22].
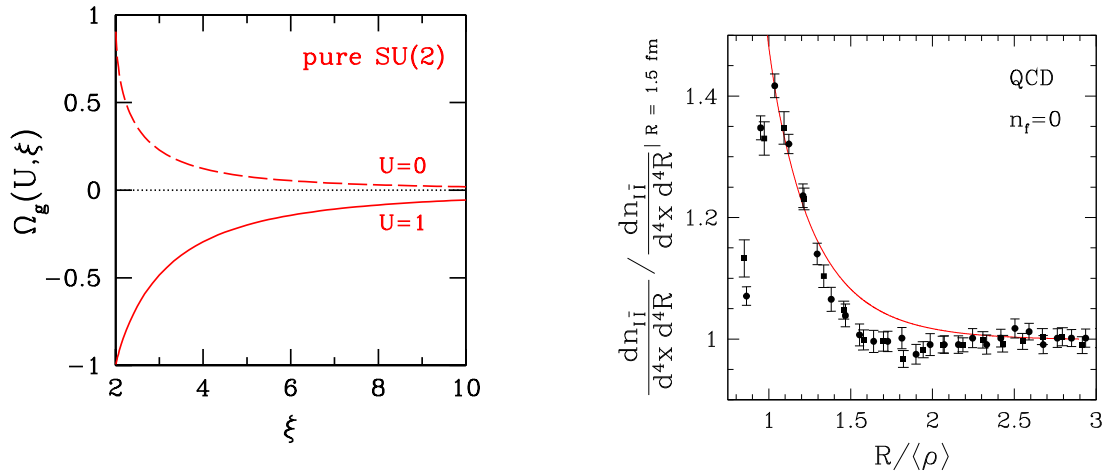
Figure 3: *Left:* $I\bar{I}$-valley interaction (2.11) as function of conformal separation ξ (2.13) for the most attractive relative orientation ($U = 1$, solid) and the most repulsive relative orientation ($U = 0$, dashed). *Right:* Illustration of the agreement of recent high-quality lattice data [28] for the $I\bar{I}$-distance distribution with the predictions from instanton-perturbation theory (solid) for $R/\rho \geq 1.05$ [22, 25].

$R < (\rho + \bar{\rho})/2$, the extraction of the $I\bar{I}$-distance distribution from the quenched QCD lattice data is quite ambiguous since there is no principal distinction between a trivial gauge field fluctuation and an $I\bar{I}$-pair at small separation. This is reflected in a considerable dependence on the cooling method/amount used to infer properties of the $I\bar{I}$-distance distribution [46, 48]. A simple extrapolation of lattice results on the topological structure of quenched $SU(2)$ gauge theory [46] to zero "cooling radius" indicates $\langle R/(\rho + \bar{\rho})/2 \rangle \approx 0.5$, i.e. strongly overlapping $I\bar{I}$-pairs in the vacuum, unlike Fig. 3 (right). Therefore, the fiducial region $R^2/(\rho\bar{\rho}) \geq 1$ for the reliability of instanton-perturbation theory inferred from lattice data should be considered as quite conservative.

2.2 Saddle-point evaluation

For weak-coupling, $\alpha_g \ll 1$, the collective coordinate integrals in the cross-section (2.4) can be performed in the saddle-point approximation, the relevant effective exponent being[4]

$$-\Gamma \equiv i\,(p_1 + p_2) \cdot R \tag{2.14}$$

$$-\begin{cases} \frac{4\pi}{\alpha_W(\mu)}\left[1 + \frac{1}{4}M_W^2(\rho^2 + \bar{\rho}^2) + \Omega_g\left(U, \frac{R^2}{\rho\bar{\rho}}, \frac{\bar{\rho}}{\rho}\right)\right] & [\text{QFD } (p_1^2 = p_2^2 = 0)], \\ Q'\,(\rho + \bar{\rho}) + \frac{4\pi}{\alpha_s(\mu)}\left[1 + \Omega_g\left(U, \frac{R^2}{\rho\bar{\rho}}, \frac{\bar{\rho}}{\rho}\right)\right] & [\text{QCD (DIS: } -p_1^2 = Q'^2 > 0, p_2^2 = 0)]. \end{cases}$$

---

[4]In the case of QCD, some additional terms, which arise from the running of α_s and are formally of pre-exponential nature, have to be included in Eqs. (2.14) and (2.15) for numerical accuracy [21]. The simplified expressions (2.14), (2.15) suffice, however, for illustrative purposes and are numerically adequate for QFD.

For the case of QFD, the Higgs part Ω_h of the $I\bar{I}$-interaction has been neglected in (2.14) and for the gauge part the one from the pure gauge theory, Ω_g, was taken. This should be considered as reliable as long as the dominant contribution to the QFD instanton-induced cross-section is due to the multiple production of $\mathcal{O}(1/\alpha_g)$ transverse W's and Z's – as is the case at energies below the sphaleron (2.1) – rather than of longitudinal ones and of Higgs bosons [12].

The saddle-point equations, $\partial\Gamma/\partial\chi_{|\chi_*} = 0$, with $\chi = \{U, R, \rho, \bar{\rho}\}$, following from (2.14) imply that the instantons and anti-instantons contributing to the cross-section (2.4) are dominantly in the most attractive relative orientation, $U_* = 1$, and tend to have equal sizes, $\rho_* = \bar{\rho}_*$. The remaining equations, determining $(R/\rho)_*$ and ρ_*, can be summarized as[4]

$$\left(\frac{R}{\rho}\right)_* = M_W \rho_* \left(\frac{4\pi M_W/\alpha_W}{\sqrt{\hat{s}}}\right), \, \frac{(M_W \rho_*)^2}{2} = \left[(\xi_* - 2)\frac{\partial}{\partial\xi_*}\Omega_g(1, \xi_*)\right]_{|\xi_* = 2 + \left(\frac{R}{\rho}\right)_*^2} \text{(QFD)},$$
(2.15)

$$\left(\frac{R}{\rho}\right)_* = 2\frac{Q'}{\sqrt{\hat{s}}}, \, Q'\rho_* = \frac{4\pi}{\alpha_s}\left[(\xi_* - 2)\frac{\partial}{\partial\xi_*}\Omega_g(1, \xi_*)\right]_{|\xi_* = 2 + \left(\frac{R}{\rho}\right)_*^2} \text{(QCD)},$$

where $(p_1 + p_2)^2 = \hat{s}$ denotes the parton-parton center-of-mass (cm) energy. To exponential accuracy ($\alpha_g \ll 1$), the cross-section (2.4) is then given by

$$\hat{\sigma}^{(I)} \propto \mathrm{e}^{-\Gamma_*} \equiv \mathrm{e}^{-\frac{4\pi}{\alpha_g}F_g(\epsilon)}, \tag{2.16}$$

where

$$\epsilon = \begin{cases} \frac{\sqrt{\hat{s}}}{4\pi M_W/\alpha_W} & \text{in QFD}, \\ \frac{\sqrt{\hat{s}}}{Q'} & \text{in QCD}, \end{cases} \tag{2.17}$$

is a scaled cm energy and

$$F_g = \begin{cases} \left[1 + \Omega_g(1, \xi_*) - (\xi_* - 2)\frac{\partial}{\partial\xi_*}\Omega_g(1, \xi_*)\right]_{|\xi_* = 2 + \left(\frac{R}{\rho}\right)_*^2} & \text{in QFD}, \\ [1 + \Omega_g(1, \xi_*)]_{|\xi_* = 2 + \left(\frac{R}{\rho}\right)_*^2} & \text{in QCD}. \end{cases} \tag{2.18}$$

is the "holy-grail function [17]", determining the fate of instanton-induced hard scattering processes at high energies.

Both in QFD as well as in QCD, the prediction (2.18) for the holy-grail function $F_g(\epsilon)$ decreases monotonically for increasing scaled energy ϵ from its value at zero energy, $F_g(0) = 1$. It approaches zero, $F_g \to 0$, at asymptotic energies, $\epsilon \to \infty$ (cf. Fig. 4 (middle)). In other words, at all finite energies, the cross-section (2.16) is formally exponentially suppressed and there is no apparent problem with unitarity [7]. It should be noticed, however, that at high cm energies the $I\bar{I}$-interaction is probed at small distances, $(R/\rho)_* \sim 1$ (cf. Fig. 4 (top)), making the semi-classical and saddle-point evaluation unreliable. In this connection, the information on the fiducial region in $R/\langle\rho\rangle$ of the instanton-perturbative description from QCD lattice simulations (cf. Fig. 3 (right)) can be most appreciated. Note furthermore
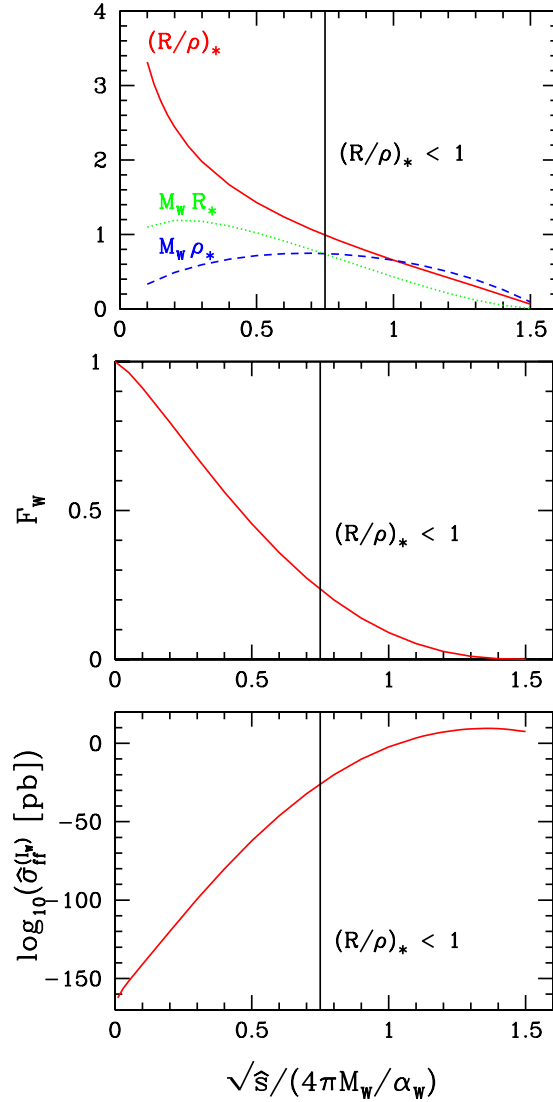
Figure 4: QFD instanton subprocess cross-section related quantities, as function of scaled parton-parton center-of-mass energy $\sqrt{\hat{s}}/(4\pi M_W/\alpha_W)$. *Top:* Saddle point values for collective coordinates [12]. *Middle:* Holy-grail function, $\hat{\sigma}^{(I_W)} \propto \exp[-(4\pi/\alpha_W)\,F_W]$ [12]. *Bottom:* Total cross-section $\hat{\sigma}_{\mathrm{ff}}^{(I_W)}$ for QFD instanton-induced fermion-fermion scattering, $\mathrm{f} + \mathrm{f} \xrightarrow{I_W} \mathrm{all}$ [29]. It stays unobservably small, $\hat{\sigma}_{\mathrm{ff}}^{(I_W)} \le 10^{-26}$ pb, in the conservative fiducial kinematical region corresponding to $(R/\rho)_* \ge 1$ inferred via the QFD–QCD analogy from lattice data and HERA. If one allows, however, for a slight extrapolation towards smaller $(R/\rho)_* \approx 0.7$, the prediction rises to $\hat{\sigma}_{\mathrm{ff}}^{(I_W)} \approx 10^{-6}$ pb.

that, in the case of QFD, $M_W R_* \lesssim 1$ in the whole energy range considered in Fig. 4 (top), justifying a posteriori the approximation of the full valley interaction in QFD by the one
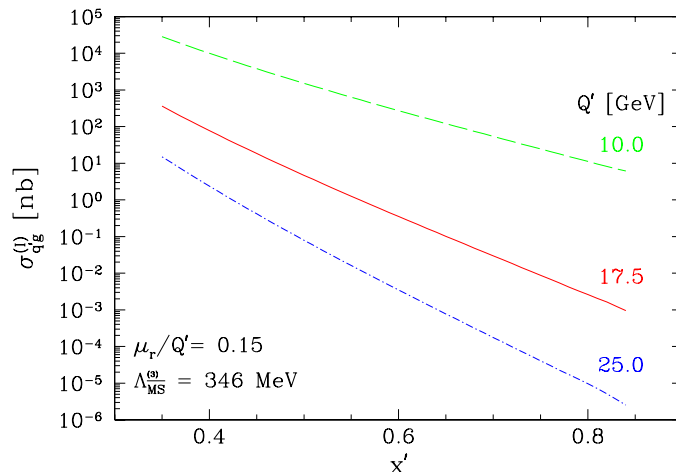
Figure 5: Total cross-section for the QCD instanton quark-gluon initiated subprocess in Fig. 1 (right), as a function of the Bjorken variable $x' = Q'^2/(Q'^2 + \hat{s})$, for different values of the virtuality Q' [21, 24].

from the pure gauge theory, Ω_g.

The energy dependences of the instanton-induced parton-parton cross sections illustrated in Fig. 4 (bottom) for QFD [29] and in Fig. 5 for QCD in DIS [21, 24] are easily understood on the basis of the saddle-point relations above: At increasing energies, smaller and smaller $I\bar{I}$-distances are probed (cf. Fig. 4 (top)), and the cross-sections are rapidly growing due to the attractive nature of the $I\bar{I}$-interaction in the perturbative semi-classical regime (cf. Fig. 3 (left)). Furthermore, in the case of DIS, at increasing virtuality Q' smaller and smaller instantons are probed and the cross-section diminishes in accord with the size distribution (cf. Fig. 2 (right)).

3. QCD-instantons at HERA

Meanwhile, the results of a first dedicated search for QCD instanton-induced processes in DIS have been published by the H1 collaboration [26]. For this search, the theory and phenomenology of hard QCD instanton-induced processes in DIS developed by Fridger Schrempp and myself [19, 20, 21, 22, 23, 24, 25] has been used extensively. Several observables characterising the hadronic final state of QCD instanton-induced events (cf. Fig. 6) were exploited to identify a potentially instanton-enriched domain. The results obtained are intriguing but non-conclusive. An excess of events with instanton-like topology over the expectation of the standard DIS background is observed, which, moreover, is compatible with the instanton signal (cf. Fig. 7). After combinatorial cuts on instanton-sensitive observables, which suppress the background by about a factor of $\mathcal{O}(10^3)$, 484 events are found in the data, while the standard DIS background Monte Carlo simulations MEPS and CDM predict 304^{+21}_{-25} and 443^{+29}_{-35}, respectively[5]. However, the observed excess can not be claimed to be significant given the uncertainty of the Monte Carlo simulations of the standard DIS

---

[5] The quoted errors on the expected event numbers include the statistical and the experimental systematic uncertainties. For details about MEPS and CDM, see Ref. [26]
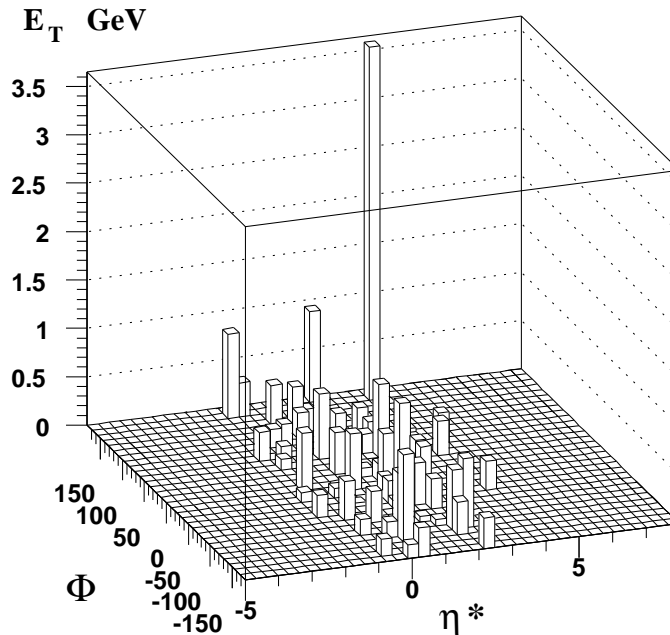
Figure 6: Distribution of the transverse energy E_T in the pseudo-rapidity (η) azimuthal (Φ) plane in the hadronic cm system for a typical QCD instanton-induced event at HERA, generated by QCDINS [24] after typical detector cuts (from [23]). Clearly recognizable are the current jet at $\eta \simeq 3, \Phi = 160^{O}$ and the "instanton band" at $0 \overset{<}{\sim} \eta \overset{<}{\sim} 2$, the latter reflecting the isotropic multi-particle nature of an instanton-induced final state.

background. Therefore, only upper limits on the cross-section for QCD instanton-induced processes are set, dependent on the kinematic domain considered [26]. From this analysis one may infer, via the saddle point correspondence, that the cross-section calculated within instanton-perturbation theory is ruled out for $(R/\rho)_* \lesssim 0.84$, in a range 0.31 fm $\lesssim \rho_* \lesssim 0.33$ fm of effective instanton sizes [29]. It should be kept in mind, however, that in the corresponding – with present statistics accessible – kinematical range the running coupling is quite large, $\alpha_s(\rho_*^{-1}) \approx 0.4$, and one is therefore not very sensitive[6] to the $I\bar{I}$-interaction, which appears in the exponent with coefficient $4\pi/\alpha_s \approx 31$. Instanton-induced rates in QFD, on the other hand, are extremely sensitive to Ω, since $4\pi/\alpha_W \approx 372$. An extension of the present H1 limit on $(R/\rho)_*$ towards smaller ρ_* and $\alpha_s(\rho_*^{-1})$, which should be possible with increased statistics at HERA II, would be very welcome. At present, the data do not exclude the cross-section predicted by instanton-perturbation theory for small $(R/\rho)_* \gtrsim 0.5$, as long as one probes only very small instanton-sizes $\rho_* \ll 0.3$ fm.

4. QFD-instantons at VLHC?

Let us finally discuss the result of a state of the art evaluation of the cross-section (2.4) for QFD [29], including all the prefactors – an analogous evaluation has been presented for

---

[6]This is of course welcome for the QCD instanton searches at HERA, because it makes predictions for the bulk of data quite reliable.
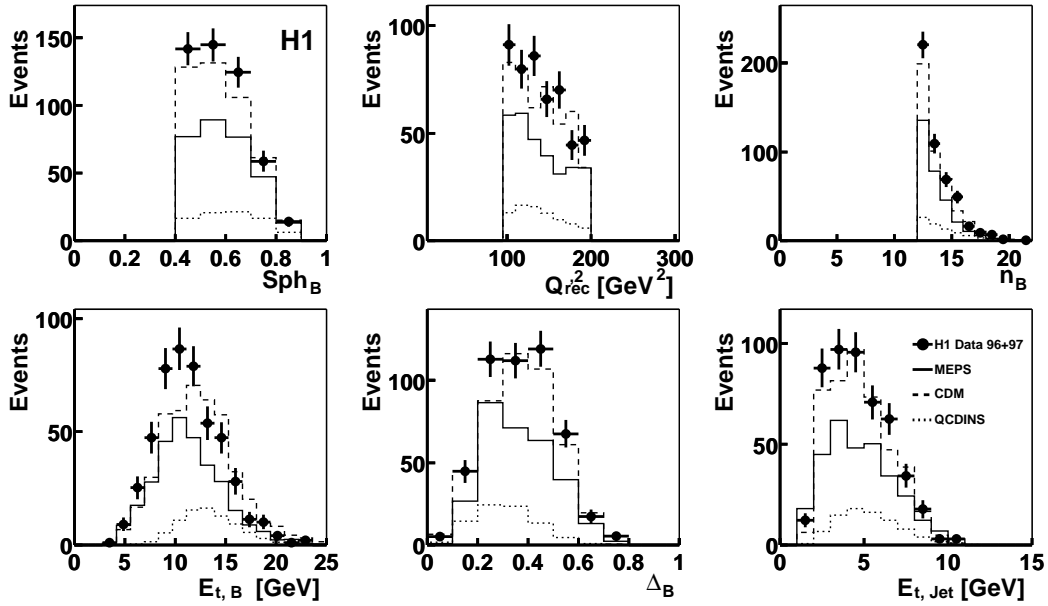
Figure 7: Distributions of DIS final-state observables (cf. Fig. 6) after combinatorial cuts, as measured by the H1 collaboration at HERA [26]. *Upper panel from left to right: a)* Sphericity in the instanton band, *b)* reconstructed virtuality, *c)* charged particle multiplicity in the instanton band. *Lower panel from left to right: d)* transverse energy in the instanton band, *e)* isotropy variable, *f)* transverse energy of current jet. Data (filled circles), the predictions from the standard DIS Monte Carlo simulations MEPS and CDM (solid and dashed line, respectively) and from the QCD instanton Monte Carlo simulation QCDINS [24] (dotted) are shown. The data exhibit an excess over the predictions from MEPS and CDM, which is compatibel with the instanton signal. In view of the uncertainties of the prediction of the standard DIS background, the excess can not be claimed to be significant, however.

QCD in DIS in Ref. [21]. The prediction[7] for the QFD instanton-induced fermion-fermion cross-section – as relevant at VLHC at the parton level – is displayed in Fig. 4 (bottom) as a function of the scaled fermion-fermion cm energy $\epsilon = \sqrt{\hat{s}}/(4\pi M_W/\alpha_W)$, for a choice $\mu = M_W$ of the renormalization scale. In the strict region of instanton-perturbation theory, $\epsilon \ll 1$, the cross-section is really tiny, e.g. $\hat{\sigma}_{\rm ff}^{(Iw)} \approx 10^{-141}$ pb at $\epsilon \approx 0.1$, but steeply growing. Nevertheless, it stays unobservably small, $\hat{\sigma}_{\rm ff}^{(Iw)} \lesssim 10^{-26}$ pb for $\epsilon \lesssim 0.75$, in the conservative fiducial kinematical region corresponding to $(R/\rho)_* \gtrsim 1$ inferred via the QFD–QCD analogy from lattice data and HERA. If one makes, however, a slight extrapolation towards smaller $(R/\rho)_* \approx 0.7$ – still compatible with lattice results and HERA – the prediction[7] rises to $\hat{\sigma}_{\rm ff}^{(Iw)} \approx 10^{-6}$ pb at $\epsilon \approx 1$, corresponding to a parton-parton cm energy of about 30 TeV. In this case, QFD instanton-induced $B + L$ violating events will have observable rates at VLHC, which has a projected proton-proton cm energy of $\sqrt{s} = 200$ TeV and a luminosity of about $\mathcal{L} \approx 6 \cdot 10^5$ pb^{-1} yr^{-1} [31]. An exciting phenomenology at VLHC will emerge if this possibility is realized in nature [14, 15]. The high transverse energy of the final state, combined with the large number of high p_T leptons and the inability to resolve jets means

---

[7]At $\epsilon \sim 1$ it should be rather called an educated extrapolation or guess.

that any conventional Standard Model background can be easily separated. While the prospects to directly verify B violation are poor, the verification of L violation seems to be possible if one succeeds in collecting a sample of $10^{2 \div 3}$ QFD instanton-induced events [15].

Let us finally speculate about the possibility that the prediction[7] in Fig. 4 (bottom) is valid even at higher energies, corresponding to even smaller $(R/\rho)_*$. In this case, we can expect to be able to see the first signs of electroweak sphaleron production in present day or near future cosmic ray facilities and neutrino telescopes [16], even before the commissioning of VLHC.

In the meantime, we have a lot of opportunities to improve our understanding of QCD instantons on the lattice and in deep-inelastic scattering at HERA, with important implications also for QFD instantons at very high energies.

Acknowledgments

References

[1] S. L. Adler, Phys. Rev. **177** (1969) 2426; J. S. Bell and R. Jackiw, Nuovo Cim. A **60** (1969) 47; W. A. Bardeen, Phys. Rev. **184** (1969) 1848.

[2] G. 't Hooft, Phys. Rev. Lett. **37** (1976) 8; Phys. Rev. D **14** (1976) 3432 [Erratum-ibid. D **18** (1978) 2199].

[3] A. Belavin, A. Polyakov, A. Shvarts and Y. Tyupkin, Phys. Lett. B **59** (1975) 85.

[4] E. V. Shuryak, Nucl. Phys. B **203** (1982) 93; D. Diakonov and V. Y. Petrov, Phys. Lett. B **147** (1984) 351; Nucl. Phys. B **272** (1986) 457.

[5] T. Schäfer and E. V. Shuryak, Rev. Mod. Phys. **70** (1998) 323; H. Forkel, arXiv:hep-ph/0009136; D. Diakonov, arXiv:hep-ph/0212026.

[6] V. A. Kuzmin, V. A. Rubakov and M. E. Shaposhnikov, Phys. Lett. B **155** (1985) 36; P. Arnold and L. D. McLerran, Phys. Rev. D **36** (1987) 581; A. Ringwald, Phys. Lett. B **201** (1988) 510.

[7] V. A. Rubakov and M. E. Shaposhnikov, Usp. Fiz. Nauk **166** (1996) 493 [Phys. Usp. **39** (1996) 461].

[8] H. Aoyama and H. Goldberg, Phys. Lett. B **188** (1987) 506.

[9] A. Ringwald, Nucl. Phys. B **330** (1990) 1; O. Espinosa, Nucl. Phys. B **343** (1990) 310.

[10] L. D. McLerran, A. I. Vainshtein and M. B. Voloshin, Phys. Rev. D **42** (1990) 171; J. M. Cornwall, Phys. Lett. B **243** (1990) 271; P. B. Arnold and M. P. Mattis, Phys. Rev. D **42** (1990) 1738; S. Y. Khlebnikov, V. A. Rubakov and P. G. Tinyakov, Nucl. Phys. B **347** (1990) 783; *ibid.* B **350** (1991) 441; A. H. Mueller, Nucl. Phys. B **348** (1991) 310; *ibid.* B **353** (1991) 44; A. Ringwald and C. Wetterich, Nucl. Phys. B **353** (1991) 303; M. Maggiore and

M. A. Shifman, Nucl. Phys. B **371** (1992) 177; V. V. Khoze, J. Kripfganz and A. Ringwald, Phys. Lett. B **275** (1992) 381 [Erratum-ibid. B **279** (1992) 429]; *ibid.* B **277** (1992) 496; A. Ringwald, Phys. Lett. B **285** (1992) 113; V. A. Rubakov, D. T. Son and P. G. Tinyakov, Phys. Lett. B **287** (1992) 342; D. Diakonov and V. Petrov, Phys. Rev. D **50** (1994) 266; F. Bezrukov, C. Rebbi, V. Rubakov and P. Tinyakov, arXiv:hep-ph/0110109.

[11] V. I. Zakharov, Nucl. Phys. B **371** (1992) 637; M. Porrati, Nucl. Phys. B **347** (1990) 371; V. V. Khoze and A. Ringwald, Nucl. Phys. B **355** (1991) 351.

[12] V. V. Khoze and A. Ringwald, Phys. Lett. B **259** (1991) 106.

[13] E. V. Shuryak and J. J. Verbaarschot, Phys. Rev. Lett. **68** (1992) 2576.

[14] G. R. Farrar and R.-b. Meng, Phys. Rev. Lett. **65** (1990) 3377; A. Ringwald, F. Schrempp and C. Wetterich, Nucl. Phys. B **365** (1991) 3.

[15] M. J. Gibbs, A. Ringwald, B. R. Webber and J. T. Zadrozny, Z. Phys. C **66** (1995) 285; M. J. Gibbs and B. R. Webber, Comput. Phys. Commun. **90** (1995) 369.

[16] D. A. Morris and R. Rosenfeld, Phys. Rev. D **44** (1991) 3530; D. A. Morris and A. Ringwald, Astropart. Phys. **2** (1994) 43.

[17] M. P. Mattis, Phys. Rept. **214** (1992) 159; P. G. Tinyakov, Int. J. Mod. Phys. A **8** (1993) 1823; R. Guida, K. Konishi and N. Magnoli, Int. J. Mod. Phys. A **9** (1994) 795.

[18] I. I. Balitsky and V. M. Braun, Phys. Lett. B **314** (1993) 237.

[19] A. Ringwald and F. Schrempp, in *Quarks '94*, Vladimir, Russia, 1994, arXiv:hep-ph/9411217.

[20] S. Moch, A. Ringwald and F. Schrempp, Nucl. Phys. B **507** (1997) 134.

[21] A. Ringwald and F. Schrempp, Phys. Lett. B **438** (1998) 217.

[22] A. Ringwald and F. Schrempp, Phys. Lett. B **459** (1999) 249.

[23] T. Carli, J. Gerigk, A. Ringwald and F. Schrempp, in: Monte Carlo Generators for HERA Physics, Hamburg, Germany, 27-30 Apr 1998, arXiv:hep-ph/9906441.

[24] A. Ringwald and F. Schrempp, Comput. Phys. Commun. **132** (2000) 267.

[25] A. Ringwald and F. Schrempp, Phys. Lett. B **503** (2001) 331.

[26] C. Adloff *et al.* [H1 Collaboration], Eur. Phys. J. C **25** (2002) 495.

[27] D. E. Kharzeev, Y. V. Kovchegov and E. Levin, Nucl. Phys. A **690** (2001) 621; M. A. Nowak, E. V. Shuryak and I. Zahed, Phys. Rev. D **64** (2001) 034008; F. Schrempp, J. Phys. G **28** (2002) 915; F. Schrempp and A. Utermann, Acta Phys. Polon. B **33** (2002) 3633; Phys. Lett. B **543** (2002) 197; arXiv:hep-ph/0301177.

[28] D. A. Smith and M. J. Teper [UKQCD collaboration], Phys. Rev. D **58** (1998) 014505.

[29] A. Ringwald, Phys. Lett. B **555** (2003) 227.

[30] The Eurasian Long Intersecting Storage Ring (ELOISATRON), http://emcsc.ccsem.infn.it/ELN.html

[31] The Very Large Hadron Collider (VLHC), http://www.vlhc.org

[32] I. Affleck, Nucl. Phys. B **191** (1981) 429.

[33] R. Jackiw and C. Rebbi, Phys. Rev. Lett. **37** (1976) 172; C. G. Callan, R. F. Dashen and D. J. Gross, Phys. Lett. B **63** (1976) 334.

PrHEP JHW2002

[34] F. R. Klinkhamer and N. S. Manton, Phys. Rev. D **30** (1984) 2212.

[35] F. R. Klinkhamer, Nucl. Phys. B **376** (1992) 255; *ibid.* B **407** (1993) 88.

[36] I. I. Balitsky and V. M. Braun, Phys. Rev. D **47** (1993) 1879.

[37] A. V. Yung, Nucl. Phys. B **297** (1988) 47.

[38] J. J. Verbaarschot, Nucl. Phys. B **362** (1991) 33 [Erratum-ibid. B **386** (1992) 236].

[39] P. B. Arnold and M. P. Mattis, Phys. Rev. D **44** (1991) 3650; A. H. Mueller, Nucl. Phys. B **364** (1991) 109; D. Diakonov and V. Petrov, in *26th LNPI Winter School*, Leningrad, 1991, pp. 8-64; D. Diakonov and M. V. Polyakov, Nucl. Phys. B **389** (1993) 109; I. Balitsky and A. Schäfer, Nucl. Phys. B **404** (1993) 639.

[40] C. W. Bernard, Phys. Rev. D **19** (1979) 3013.

[41] T. R. Morris, D. A. Ross and C. T. Sachrajda, Nucl. Phys. B **255** (1985) 115.

[42] K. Hagiwara *et al.* [Particle Data Group Collaboration], Phys. Rev. D **66** (2002) 010001.

[43] A. Hasenfratz and P. Hasenfratz, Nucl. Phys. B **193** (1981) 210; M. Lüscher, Nucl. Phys. B **205** (1982) 483; G. 't Hooft, Phys. Rept. **142** (1986) 357.

[44] S. Capitani, M. Lüscher, R. Sommer and H. Wittig [ALPHA Collaboration], Nucl. Phys. B **544** (1999) 669.

[45] A. Hasenfratz and C. Nieter, Phys. Lett. B **439** (1998) 366.

[46] M. Garcia Perez, O. Philipsen and I. O. Stamatescu, Nucl. Phys. B **551** (1999) 293.

[47] J. W. Negele, Nucl. Phys. Proc. Suppl. **73** (1999) 92; M. Teper, Nucl. Phys. Proc. Suppl. **83** (2000) 146.

[48] I. O. Stamatescu, arXiv:hep-lat/0002005.

[49] E. V. Shuryak, arXiv:hep-ph/9909458.